A LETTERS JOURNAL EXPLORING
THE FRONTIERS OF PHYSICS

OFFPRINT

Helicity and broken symmetry of DNA-nanotube hybrids

V. I. PULLER and S. V. ROTKIN

EPL, **77** (2007) 27006

A Letters Journal Exploring the Frontiers of Physics

January 2007

EPL, **77** (2007) 27006
doi: 10.1209/0295-5075/77/27006

www.epljournal.org

Helicity and broken symmetry of DNA-nanotube hybrids

V. I. Puller[1] and S. V. Rotkin[1,2(a)]

[1] *Physics Department, Lehigh University - 16 Memorial E Dr., Bethlehem, PA 18015, USA*
[2] *Center for Advanced Materials and Nanotechnology, Lehigh University - 5 E.Packer Ave., Bethlehem PA 18015, USA*

received 28 September 2006; accepted in final form 23 November 2006
published online 18 January 2007

PACS 73.22.-f – Electronic structure of nanoscale materials: clusters, nanoparticles, nanotubes, and nanocrystals
PACS 87.14.Gg – DNA, RNA
PACS 03.65.Pm – Relativistic wave equations

Abstract – We study breaking of the "supersymmetry" of an intrinsically achiral armchair carbon nanotube by means of a helical perturbation. Lowering of the symmetry results in the appearance of a non-zero effective mass for nanotube low-energy excitations, which otherwise are massless Dirac fermions. Other important consequences of the symmetry breaking are opening of gaps in the energy spectrum and shifting of the Fermi points, which we classify according to their functional dependence on the nanotube and helix parameters. Within each class the gaps are proportional to the inverse of the nanotube radius, and appear to be sensitive to the exact position of the helix in a unit cell. These results are of immediate importance for the study of DNA-nanotube complexes, and can be verified by means of optical/electron spectroscopy or tunneling microscopy.

The unusual material and electronic properties of carbon single-wall nanotubes (referred as NTs below) such as extraordinary strength, light weight, high conductivity, sharp optical absorption spectra and bright luminescence [1], are in the focus of interest of physicists at present. NTs hold promise for practical applications in nano-electronics and Nano-Electromechanical Systems (NEMS) [1]. Recently, a DuPont group has shown progress in synthesis of a DNA-NT complex which is used for NT separation and selective placement [2]. In this complex, single-stranded DNA is wrapped around a tube in a helical way with a fixed pitch [2] and, thus, fixed chirality, as shown in fig. 1. Similar complexes were observed in multiwall NTs in [3].

This letter addresses the vibrant question of whether the DNA-NT complex can still have the same electronic and optical properties as a pristine NT. The answer we give is, in general, *the DNA changes the band gap of the NT and thus modulates the electronic and optical properties.* To demonstrate the most dramatic changes that the DNA wrap may cause, we present the theory of the gap opening in the metallic armchair-NT (A-NT), which is a special type of NT with a "super-symmetry" [4]. The additional symmetry of the pristine A-NT is responsible for the absence of a band gap [5] and is difficult to break by a non-chiral perturbation. Thus, the A-NT is an ideal system to study the role of the DNA wrap.

The highly charged backbone of the DNA wrap [6] is the major source of perturbation to NT electronic structure. The Coulomb effects are often neglected in the literature where NTs are modeled as a lattice of non-charged carbon atoms (for example, [7]). We performed numerical modeling of DNA-NT complexes of different symmetry (to be presented elsewhere [8]) and found that a great deal of qualitative understanding of the effect can be obtained within a less computationally demanding and more physically transparent approach. The honeycomb lattice of the graphite monolayer (graphene) that constitutes the NT wall has two atoms in the unit cell, denoted as A and B below (fig. 1). Graphene is a zero-band gap semiconductor: the conduction and valence bands meet at the Fermi point, where the dispersion relation is approximately linear in momentum. Therefore the low-energy excitations of a graphene sheet or a metallic NT are conveniently described by the Dirac Hamiltonian for a massless particle [9], as detailed below. In particular, *the four crossing subbands* of a metallic NT are given by the Hamiltonian (written in momentum representation,

(a) E-mail: rotkin@lehigh.edu

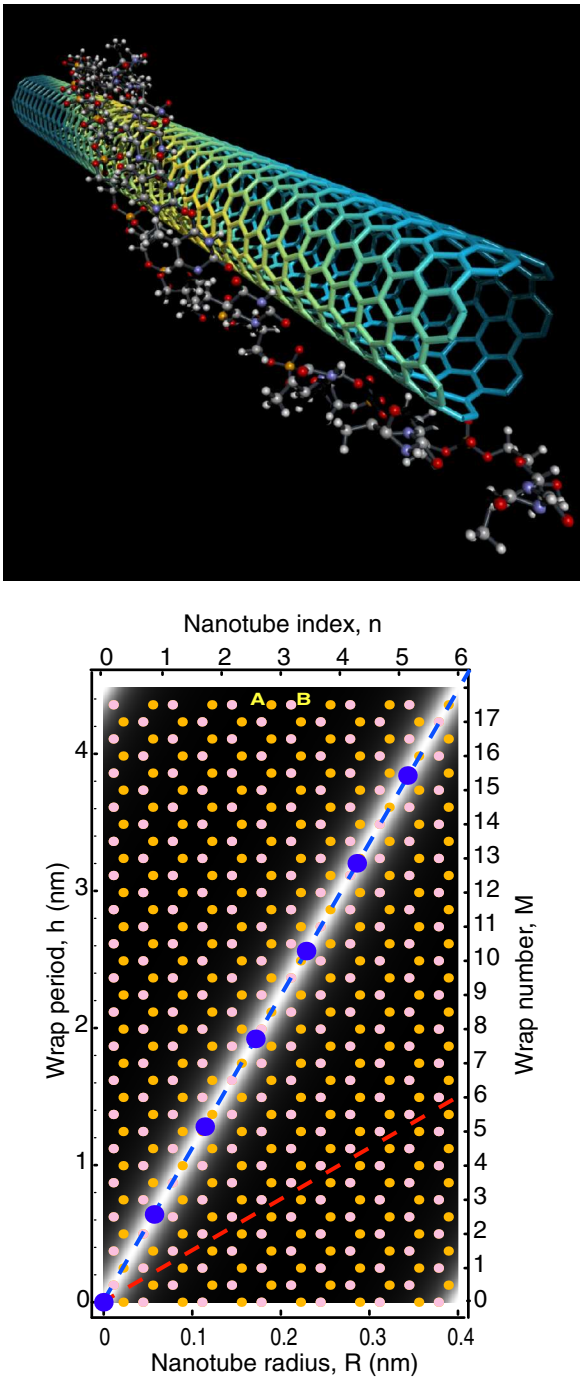

Fig. 1: (Color online) 3D view of NT wrapped by a DNA helix (top), and the envelope potential profile of the helix with the background of NT carbon network (bottom). The zigzag and armchair directions are shown with red and blue dashed lines, respectively.

in the basis $K_{+1}A, K_{+1}B, K_{-1}B, K_{-1}A$ [10])

$$\mathcal{H}_0 = vq \begin{pmatrix} \sigma_x & 0 \\ 0 & -\sigma_x \end{pmatrix} = vq\Pi_z \otimes \sigma_x, \qquad (1)$$

where $\Pi_x, \Pi_y, \Pi_z, I_\Pi$ are Pauli matrices and a unit matrix that operate in K-point space (space of two Fermi-points: $K_{\pm 1} = \pm 2\pi/(3\sqrt{3}b)$), whereas $\sigma_x, \sigma_y, \sigma_z, I_\sigma$ are the Pauli

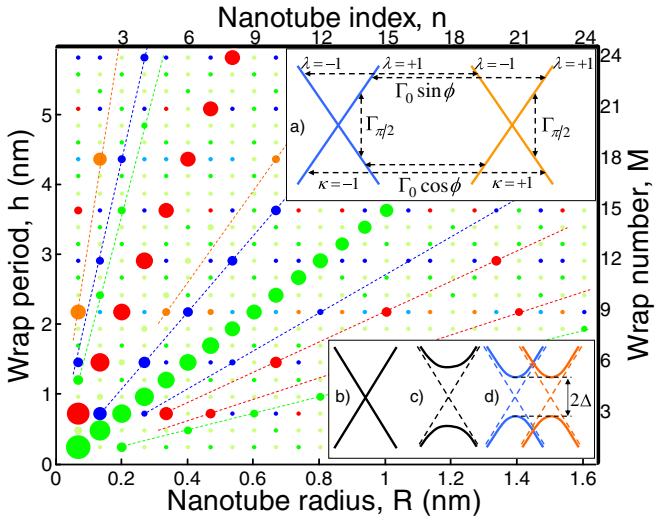

Fig. 2: (Color online) Size of the linear gap due to a helical perturbation as a function of the indices M and n. The diameter of a circle is proportional to the gap value. Color assignment for the symmetry breaking mechanisms is as follows: green - (Ze); light green - (Zo); light blue - (A1e); blue - (A2e); orange - (A1o); red - (A2o). The insets show: (a) a schematic representation of the states of Hamiltonian $\mathcal{H}_0$ and the transitions induced by a helical perturbation; (b) the energy diagram for NT without perturbation, (c) NT with perturbation of type (Z) or (A1), and (d) NT with perturbation of type (A2).

matrices and the unit matrix that operate in AB space (space of sublattices A and B) [11]; q is the electron momentum along the NT measured from the Fermi points: $\hbar k = \hbar K + q$; v is Fermi velocity, $v \simeq 9 \times 10^7$cm/s, and $b \simeq 1.4$ Å is the carbon-carbon bond length. One needs two different pseudo-spin operators, $\vec{\Pi}$ and $\vec{\sigma}$, because there are four fermion species in the NT bands at the energies close to the Fermi level. The eigenenergies and eigenstates for the Hamiltonian (1) are schematically shown in fig. 2a (inset).

The purpose of this letter is to derive the effect of the symmetry breaking due to a DNA/polymer molecule wrapped in a helical fashion around a NT and to compute the resulting gap opening. The DNA/polymer is modeled as a long homogeneous line of charge wrapped around the NT, and the period of the helix along the NT axis is assumed to be commensurate[1] with the NT unit cell length. If, for a moment, we assume that the coordinate origin for the helix coincides with one of the NT atoms, which belongs, *e.g.*, to the sublattice A, then, as we move along the helix, we pass through other NT atoms, which belong either to the same sublattice (AAAAA), or to both sublattices alternately (ABABABA). Surprisingly, all helices fall into one of the two categories.

[1]Commensurate wrap symmetry is not exhausted by the wraps with a single helix pitch per translational period h. The wraps with Q winds per M unit cells of the NT form a general set of $\{M/Q, n\}$ rational helixes. Such helix can be chosen arbitrarily close to any incommensurate wrap.

The best example of the former, to which we will refer as "class (Z)", is a helix running along the zigzag direction at an angle $\alpha = \pi/6$ with respect to the circumference, whereas the best example for the latter, which we term "class (A)", is the helix running along an armchair direction at the angle $\alpha = \pi/3$ (see fig. 1). It is shown below that, among the perturbations of their class, these two sample wraps exhibit the largest gaps.

A perturbation of type (Z) breaks the symmetry with respect to interchange of the two sublattices and has the form $\Pi_z \otimes \sigma_z$. The perturbation of type (A) affects both sublattices in the same way, and cannot break the sublattice symmetry, but mixes the fermion species at K_{+1} and K_{-1}; therefore it has the form $\Pi_x \otimes \sigma_x$.

We now part with the assumption that the coordinate origin for the helix coincides with a carbon atom, and write the general form of the perturbation Hamiltonian as

$$\mathcal{H}_1 + \delta\mathcal{H} = \Delta_0 C_0 I_\Pi \otimes I_\sigma + \Delta_0 \Gamma_\omega U_\omega \Pi_x \otimes \sigma_x U_\omega^+, \qquad (2)$$

where $\mathcal{H}_1 = \Delta_0 C_0 I_\Pi \otimes I_\sigma$ shifts the energy origin, Δ_0 is the normalized amplitude of the potential of the DNA backbone to be derived in eq. (5), and C_0 and Γ_ω depend on the symmetry of the DNA-NT hybrid. $U_\omega = u_z(\phi)U_y(\omega)u_y(\omega)$ is a rotation in $SU(2) \otimes SU(2)$ space[2], $U_j(\chi) = e^{i\chi\Pi_j/2}$, and $u_j(\chi) = e^{i\chi\sigma_j/2}$. For the helices commensurate with a NT translational period, the phase ω can take only two values: $\omega = \pi/2$, and $\omega = 0$, corresponding to cases (Z) and (A), respectively. It will be shown that the phase ϕ determines the shift of the Fermi points, and takes only the values: 0 and $\pm 2\pi/3$. Below we refer to these two cases as classes (A1) and (A2), respectively.

The energy spectra for the unperturbed Hamiltonian and for cases (Z) and (A) are shown in the insets to fig. 2.

The helical perturbations do not commute with the pseudospin-flip operator, $\Pi_x \otimes \sigma_z$, and break the valley degeneracy [10]. The projection of the "spin" onto the NT axis, $\Sigma_a = I_\Pi \otimes \sigma_x$, is preserved only by a perturbation of type (A1), and therefore is not a convenient characteristic of symmetry breaking. Perturbations of type (Z) and (A) can be distinguished by whether "K-spin", κ, is preserved. The operator of "K-spin" is $\mathcal{K} = \Pi_z \otimes I_\sigma$, and for a perturbation of type (Z) ($\omega = \pi/2$) it commutes with the total Hamiltonian, $\mathcal{H}_0 + \mathcal{H}_1 + \delta\mathcal{H}$. The eigenfunctions of $\mathcal{H}_0$ corresponding to definite values of $\kappa = \pm 1$, $\Psi_{\lambda,\kappa}$ are given by $\Psi_{\lambda,+1} = (1, \lambda, 0, 0)^T/\sqrt{2}$, and $\Psi_{\lambda,-1} = (0, 0, 1, -\lambda)^T/\sqrt{2}$, where $\lambda = \pm 1$ is the energy index, $E_\lambda(q) = \lambda v q$. In this basis, the conservation of κ gives us a trivial result: the Hamiltonian $\mathcal{H}_0 + \mathcal{H}_1 + \delta\mathcal{H}$ is already in a block-diagonal form, and the diagonalization of the blocks corresponding to different $\kappa = \pm 1$ produces its energy spectrum as

$$E_\tau^Z(q) = \Delta_0 C_0 + \tau\sqrt{(\Delta_0\Gamma_{\pi/2})^2 + v^2 q^2}, \qquad (3)$$

where $\tau = \pm 1$ labels new conduction and valence bands. This spectrum is twice degenerate in κ, and has a gap of width $2\Delta = 2\Delta_0|\Gamma_{\pi/2}|$.

The operator which commutes with $\mathcal{H}_0 + \mathcal{H}_1$ and $\delta\mathcal{H}$ in case (A) ($\omega = 0$) is $\Pi_y \otimes \sigma_z$, similar to the pseudospin-flip operator mentioned earlier. The eigenfunctions of this operator, which are simultaneously eigenfunctions of $\mathcal{H}_0$, are $\Phi_{\lambda,\rho} = (1, \lambda, i\rho, -i\rho\lambda)^T/2$. The Hamiltonian $\mathcal{H}_0 + \mathcal{H}_1 + \delta\mathcal{H}$ is block-diagonal in their basis and we readily obtain its eigenvalues as

$$E_{\tau,\rho}^A(q) = \Delta_0 C_0 + \tau\sqrt{(\Delta_0\Gamma_0\cos\phi)^2 + (vq + \rho\Delta_0\Gamma_0\sin\phi)^2}, \qquad (4)$$

where $\tau, \rho = \pm 1$. The gap in this spectrum is $2\Delta = 2\Delta_0|\Gamma_0 \cos\phi|$. Non-zero ϕ means that the Fermi point, initially located at $q_F = 0$, is now split into two Fermi points located at $q_\rho = -\rho\Delta_0\Gamma_0\sin(\phi)/v$. In case (A1), $\phi = 0$, and the Fermi point does not split.

The gap opening in the pristine metallic A-NT changes the band structure qualitatively, which can be detected by optical and electron spectroscopy, in transport and tunnelling microscopy. Figure 2 shows the dependence of the size of the gap that opens in a (n, n) NT due to a helical perturbation on the NT index, n, and the wrap number, M, which determines the period of the helix, $h = Ma$ in terms of the length of the NT unit cell, $a = \sqrt{3}b = 2.4$ Å. Although the gap opens virtually for any combination $\{n, M\}$, one can clearly notice several leading sequences, corresponding to the same ratio n/M (same helical angle α). Thus, each sequence can be labeled by a pair $\{\bar{n}, \bar{M}\}$, which do not have common divisors, or, equivalently, by the helical angle: $\tan\alpha = \bar{M}/(\bar{n}\sqrt{3})$. The two most pronounced gap sequences correspond to the series $\{1, 1\}$ ($\alpha = \pi/6$), and $\{1, 3\}$ ($\alpha = \pi/3$), which are the helices directed along the zigzag and armchair directions. The gaps in the same sequence are inversely proportional to the NT radius: $\Delta \sim 1/R$.

Numbers $\{\bar{n}, \bar{M}\}$, apart from their definitions as $\{n, M\}$ reduced by their greatest common divisor, have additional meaning from the point of view of the NT symmetry: they specify the screw symmetry that remains after the NT is wrapped by the helix: rotation about the NT axis by an angle $2\pi/(n/\bar{n})$ together with translation by $M/\bar{M}$ NT periods, *i.e.*, they specify the unit cell of the DNA-NT hybrid.

The potential of the DNA is assumed to be homogeneous along the helix and to have Lorentzian shape, $V(x)$, in the direction perpendicular to the helix, with its Fourier transform given by $\tilde{V}(k) = u_0\Lambda e^{-|k|\Lambda}$, where Λ stands for the helix thickness. In the following we consider only the effect linear in the perturbation potential, though the small correction by the higher-order terms of the perturbation theory can be readily obtained as in ref. [12].

[2] A gauge phase could appear (depending on the choice of the coordinate origin) but can be removed by transformation $\delta\mathcal{H}' = U_z(\varphi)^+\delta\mathcal{H}U_z(\varphi)$, a rotation about the z-axis in K-space, which commutes with Hamiltonian $\mathcal{H}_0 + \mathcal{H}_1$.

We find that there are three parameters that determine the size of the gap:

i) The shape parameter $z = \exp[-2\pi\Lambda\sqrt{\bar{M}^2+3\bar{n}^2}/(a\sqrt{3})]$ results from the finite range of the DNA potential. The argument of the exponent is the ratio of the area covered by the helix in a unit cell of DNA-NT hybrid to the area of one hexagon.

ii) The offset parameter, $x = 2\pi\bar{n}l_0/a$, characterizes the coordinate origin of the helix x_0, y_0. Here, $l_0 = x_0 - y_0\tan\alpha$ is the axial distance between the helix and C_2 rotational axis passing through the middle of a bond parallel to the circumference. The results have to be periodic functions of this parameter, since displacement of the helix along the NT by one NT period a does not alter the size of a gap.

iii) The characteristic gap scale as given by the normalized amplitude of the potential of the DNA backbone u_0

$$\Delta_0 = \frac{u_0\Lambda}{2\pi R\sin\alpha} = \frac{u_0\Lambda}{na\sqrt{3}\sin\alpha}. \tag{5}$$

Since our analytical results follow from the linear perturbation theory, all gaps are proportional to Δ_0. Since z and x depend only on the reduced parameters $\{\bar{n}, \bar{M}\}$, the gap scales as the inverse NT radius, *i.e.*, in the same way as the band gap of a pristine semiconductor NT, in contrast to the case of secondary gaps, that can be induced by deformations, for example.

Selection rules for helical perturbation. Apart from the scaling as $1/R$, the size of the gap is determined by the symmetry of the NT-helix system, that is by numbers $\{\bar{n}, \bar{M}\}$.

For a realistic potential profile of the DNA backbone charge, the shape parameter $z \ll 1$ and the leading terms of the gaps for small z values are as follows:

(Z) class, $mod(\bar{M}, 3) = \pm 1$: the gap opens according to the scenario (Z), *i.e.*, $\Delta = \Delta_0|\Gamma_{\pi/2}|$. Depending on the parity of $\bar{M} + \bar{n}$, one should distinguish two cases:

– (Ze) $mod(\bar{n} + \bar{M}, 2) = 0$, which automatically implies that $\bar{M}, \bar{n}$ are odd numbers, since otherwise they would have 2 as a common divisor. The gap is given by

$$\Delta \simeq \Delta_0\sqrt{3}z|\sin x|. \tag{6a}$$

This gap is a periodic function of the offset parameter x, and takes zero values when $l_0 = (a/(2\bar{n}))s$, where s is an arbitrary integer, *i.e.* when the helix passes through a C_2 axis.

– (Zo) if $mod(\bar{n} + \bar{M}, 2) = 1$: the gap becomes

$$\Delta \simeq \Delta_0\sqrt{3}z^2|\sin 2x|, \tag{6b}$$

and takes zero values when $l_0 = (a/(4\bar{n}))s$.

(A) class, $mod(\bar{M}, 3) = 0$: The gap opens according to the scenario (A), and $\Delta = \Delta_0|\Gamma_0\cos\phi|$. At small z, the gap formula is determined by integer numbers M_0 and n_0, defined as $\bar{M} = 3M_0$, $M_0 = 3m_0 + \mu$, and $\bar{n} = 3n_0 + \nu$, where $\nu = \pm 1$, $\mu = 0, \pm 1$. The phase ϕ, which is given by $\phi = \mu\nu 2\pi/3$, renders additional classification, depending on whether $\mu = 0$ (scenario (A1)) or not (scenario (A2)). The gap that opens in case (A2) is half of that in case (A1). The parity of $n_0 + M_0$ allows the following classification: (A1e) $mod(n_0 + M_0, 2) = 0$, and $\mu = 0$: the gap is

$$\Delta = \Delta_0 z^{\frac{2}{3}}\left(1 + z^{\frac{2}{3}}\cos 2x - \frac{1}{2}z^{\frac{4}{3}}\cos 4x\right). \tag{7a}$$

This gap is a periodic function of the offset parameter, but never decreases to zero. The oscillations of the gaps that open according to scenario (A) are in opposite phase with those from scenario (Z), which further confirms the complementary symmetry of these wraps.

(A1o) if $mod(n_0 + M_0, 2) = 1$, and $\mu = 0$ the gap is

$$\Delta = \Delta_0 z^{\frac{1}{3}}\left(1 + (-1)^{M_0}z^{\frac{1}{3}}\cos x - \frac{1}{2}z^{\frac{2}{3}}\cos 2x\right). \tag{7b}$$

(A2o, A2e) As we discussed above, the gap opening according to scenario (A2) ($\mu = \pm 1$) is accompanied by a shift of the Fermi points (the phase ϕ is non-zero). In this case the gap is half of that given by expressions (7a) and (7): $\Delta' = \Delta/2$. The Fermi points split and shift to positions (fig. 2d)

$$q_F = \pm\frac{\Delta_0|\Gamma_0\sin\phi|}{v} = \pm\frac{\sqrt{3}\Delta}{2v}. \tag{8}$$

As we have seen, the gaps that appear due to the mixing of states lying near the same Fermi point of an A-NT, (Z), are proportional to z or z^2, whereas the gaps due to mixing of the states belonging to different Fermi points, (A), are proportional to $z^{1/3}$ and $z^{2/3}$. According to the definition of the parameter z, the largest gaps are those with the smallest value of $\sqrt{\bar{M}^2 + 3\bar{n}^2}$. Thus, the largest gaps are those in the sequence $\{1, 1\}$ (*i.e.*, with $M = n$, Class (Ze)), and in the sequence $\{1, 3\}$ (*i.e.*, with $M = 3n$, Class (A2o)), see fig. 2. Because of the importance of these gaps we provide the explicit expressions for them. The gap for the $\{1, 1\}$ sequence is

$$\Delta_{1,1} = \frac{\sqrt{3}}{\pi}\frac{u_0\Lambda}{R}e^{-\frac{4\pi\Lambda}{a\sqrt{3}}}\left|\sin\left(\frac{2\pi l_0}{a}\right)\right|, \tag{9a}$$

and the gap for $\{1, 3\}$ sequence is

$$\Delta_{1,3} = \frac{1}{2\pi\sqrt{3}}\frac{u_0\Lambda}{R}e^{-\frac{4\pi\Lambda}{3a}}\left(1 - e^{-\frac{4\pi\Lambda}{3a}}\cos\left(\frac{2\pi l_0}{a}\right) - \frac{1}{2}e^{-\frac{8\pi\Lambda}{3a}}\cos\left(\frac{4\pi l_0}{a}\right)\right). \tag{9b}$$

In conclusion, we found that a DNA wrapped as a regular helix may drastically change NT band structure. As an example, we presented the analytical low-energy

theory for the band gap opening in metallic A-NTs, due to symmetry breaking. We classified all possible helical potentials (that are commensurate with the A-NT lattice) and found two major mechanisms of the symmetry breaking: pseudo-spin-flip which preserves the "K-spin" symmetry and the one which mixes the "K-spin". Main features of the gaps due to the helical potential are: 1) there are classes with same helicity of DNA wraps and similar symmetry properties; 2) within a class the gap scales as $\sim 1/R$ with the NT radius; 3) a wider helical potential (which corresponds to larger Λ in our model) results in the exponential suppression of the gap (due to averaging of the potential over the atoms lying under the helix); 4) the gaps are sensitive to rotation/shift of the helix about the NT axis. In particular, there exist two positions of the helix in the $\{1,1\}$ sequence, when the gap vanishes by symmetry: when the helix passes through the middle of the bond or the center of the hexagon. A twofold symmetry axis for the NT-helix system exists in both these cases. In contrast, the gap of the $\{1,3\}$ sequence, that opens due to scenario (A), remains even when there are two-fold rotation symmetries of A-NT left intact. Our analysis proves that this effect is due to the symmetry of the operator $\delta\mathcal{H}$ which breaks the "K-spin" degeneracy in this case but preserves the sublattice degeneracy. Although to make an estimate for the band gap opening one may need a detailed knowledge of the perturbation potential, we infer from numerical studies that typical bandgaps are of the order of few meV to few tens of meV for metallic NTs [8]. Further experimental study of the structure of the DNA on the NT would be very valuable to make accurate predictions of the band structure modulation due to nanotube functionalization [13].

The ability to perform spatial modulation of the band gap of a NT via functionalization paves the way for creating NT heterostructures and related electronic devices, at least in principle. For optical spectroscopy, the role of the DNA wrap is in developing natural optical activity, typical for chiral media, even for non-chiral pristine NTs. It is known [6] that the DNA charge may vary and depends on environmental factors such as: the type of solvent, its chemical potential and pH. The band gap in a DNA-NT hybrid is a function of the charge of the DNA backbone, thus, DNA-NT hybrids may be utilized in chemical/biological sensors.

* * *

The authors are greatly indebted to B. Grosser for generating a high-resolution image and to S. Snyder, whose numerical results, complimentary to this research, motivated significant improvements in this work, and for the help in preparation of this manuscript. The work was partially supported by NSF (No.0609050, NIRT). Partial support by NASA through the Mid-Atlantic Partnership Programm is acknowledged.

REFERENCES

[1] Dresselhaus M. S., Dresselhaus G. and Avouris Ph. (Editors), *Carbon Nanotubes: Synthesis, Structure, Properties and Applications* (Springer) 2001; Meyyapan M. (Editor), *Carbon Nanotubes: Science and Applications* (CRC) 2004; Rotkin S. V. and Subramoney S. (Editors), *Applied Physics of Carbon Nanotubes* (Springer) 2005.

[2] Zheng M. *et al.*, *Science*, **302** (2003) 1545; Zheng M. *et al.*, *Nature Mater.*, **2** (2003) 338.

[3] Takahashi H., Numao S., Bandow S. and Iijima S., *Chem. Phy. Lett.*, **418** (2006) 535.

[4] Vuković T., Milošević I. and Damnjanović M., *Phys. Rev. B*, **65** (2002) 045418.

[5] Damnjanović M., Vuković T. and Milošević I., *Solid State Commun.*, **116** (2000) 265; Saito R. *et al.*, *Phys. Rev. B*, **72** (2005) 153413.

[6] Berg J. M., Tymoczko J. L. and Stryer L., *Biochemistry*, 5th edition (W. H. Freeman) 2002.

[7] Gao H. and Kong Y., *Ann. Rev. Mater. Res.*, **34** (2004) 123.

[8] Snyder S. E. and Rotkin S. V., *JETP Lett.*, **84** (2006) 348.

[9] DiVincenzo D. P. and Mele E. J., *Phys. Rev. B*, **29** (1984) 1685; Haldane F. D. M., *Phys. Rev. Lett.*, **61** (1988) 2015; Semenoff G. W., *Phys. Rev. Lett.*, **53** (1984) 2449; Khveshchenko D. V., *Phys. Rev. Lett.*, **87** (2001) 206401.

[10] McCann E. and Fal'ko V. I., *Phys. Rev. B*, **71** (2005) 085415.

[11] Kane C. L. and Mele E. J., *Phys. Rev. Lett.*, **95** (2005) 226801; Wallace P. R., *Phys. Rev.*, **71** (1947) 622.

[12] Li Y., Ravaioli U. and Rotkin S. V., *Phys. Rev. B*, **73** (2006) 035415.

[13] Chou S. G. *et al.*, *Chem. Phys. Lett.*, **397** (2004) 296; Heller D. A. *et al.*, *Science*, **311** (2006) 508; Jeng E. S. *et al.*, *Nano Lett.*, **6** (2006) 371.